

Evaluation of the Reservoir Characteristics of Exposed Sandstone Facies of the Bhuban Formation in Sitakund Anticline, Chittagong

Md. Ashraf Ali Uzzal, Janifar Hakim Lupin*, Shakhawat Hossain and Mohammad Solaiman

Department of Geology, University of Dhaka, Dhaka 1000, Bangladesh

Manuscript received: 26 February 2023; accepted for publication: 30 November 2023

ABSTRACT: This research concentrates on characterizing the sandstone reservoir features within the Bhuban Formation exposed in the Sitakund Anticline of the Chittagong Hill Tracts. Of the lack of well-qualified reservoirs, the sandstone facies in the Bhuban Formation are considered the primary reservoir source and a significant contributor to Bangladesh's hydrocarbon reserves. The Bhuban Formation showcases a pattern of alternating sandstone and shale layers. To ascertain the existence of reservoir sandstone facies in the Bhuban Formation, the study conducts analyses of exposed structures along various outcrop sections of Bariyadhala, Chandranath, Barabkunda, and Shahasradhara. Through scrutinizing lithology, sedimentary structures, bed configuration, grain size, and reservoir characteristics of rock sequences, three distinct facies types emerge: the alternating sandstone and shale layers, channel sand, and incised valley sand. These facies types signify diverse depositional environments, with the alternating sandstone and shale layers originating from tidal flats, channel sand representing sediment fill within tidal channels, and incised valley sand indicating sediment accumulation within incised valleys. The detailed petrographic analysis underscores that the incised valley fill sand exhibits the most favorable reservoir qualities, boasting an approximate porosity of 25%. The tidal channel fill and the tidal flat deposits display 20% and 8% porosity, respectively. Both channel sand and incised valley sand showcase commendable porosity and permeability. In contrast, the sample featuring the alternation of sandstone and shale has the lowest porosity and contains randomly oriented clay minerals, predominantly Kaolinite.

Keywords: Sitakund Anticline; Bhuban Formation; Channel Sand; Petrographic Analysis; Incised Valley Sand

INTRODUCTION

The Bengal Basin is a prominent sedimentary basin with a high potential for housing hydrocarbon resources, encompassing regions like West Bengal, Assam, Tripura, and Bangladesh (Alam et al., 2003). The primary focus of exploration lies within Bangladesh's Neogene Surma Group. This is primarily due to deltaic-shallow marine sediments, resulting in a sequence of reservoir sandstones. A substantial portion of the Cenozoic sedimentary facies within the Bengal Geosyncline, approximately 6 km thick, comprises Neogene clastic deltaic sediments. These sediments are prominently visible along the fold belt structures and are well-represented in drilled wells across foredeep and fold belt areas (Bhuiyan, 1995). Over the past few decades, intensive hydrocarbon exploration efforts have led to the development of comprehensive geological and geophysical databases. The quality of sandstone reservoirs is modified by a complex interplay of factors,

including mineral composition, depositional facies, diagenetic processes, and the movement of basin fluids (Noh and Lee, 1999; Zou et al., 2012; Farhaduzzaman et al., 2015). Therefore, our current research delves into the various reservoir facies within the Sitakund Anticline, aiming to unravel their petrographic characteristics.

The Sitakund anticline exhibits an asymmetric drop in an NNW-SSE geographical direction. Faults, joints, folds, and formations - Bhuban, Bokabil, and Tipam are exposed here. Notable outcrops of the Surma Group, specifically the Bhuban and Bokabil Formations, are visible along road cuts, footpaths, hillside exposures, and tributary regions near the Bariyadhala, Shahasradhara, Chandranath temple, and Barabkunda sections. Extensive exposure of the Surma Group rocks can be witnessed on the fractured eastern and western flanks.

The presence of active petroleum systems in the Bengal basin is evident from the presence of hydrocarbons in the eastern region of Bangladesh (Basri et al., 2023). High-maturity (dry) gas accumulations are believed to be the outcome of the Oligocene Jenum Formation, which has

* Corresponding Author: Janifar Hakim Lupin
Email: j.hlupin@du.ac.bd
DOI: <https://doi.org/10.3329/dujees.v12i1.70556>

migrated from a distant section of the basin. Serving as a definitive upper sealing layer, a marine shale from the transgressive phase (Upper Marine Shale) overlays the Bokabil Formation, effectively containing the upward movement of gas. The Chittagong Tripura Fold Belt (CTFB) in Bangladesh holds considerable potential for hydrocarbon extraction. Alongside conventional prospects, unconventional targets within this region can be explored for petroleum, including zones beneath broader synclinal valleys, channel sands, clay dippers with overpressure shale in deeper subsurface zones, thinly bedded plays, and similar areas (Islam and Lupin, 2020). The Surma Group (Bhuban and Bokabil formations) is the principal reservoir for hydrocarbons. Despite gas and oil in deltaic environments, the Bengal Delta predominantly contains gas resources, with notable oil discoveries being scarce. Bangladesh currently boasts 29 gas fields, with Bibiyana and Titas ranking among the most significant. In preparation for the development of Bhuban reservoirs, managing the level of compartmentalization caused by lateral variations in depositional facies and the impact of numerous extensive “incised valleys” becomes a significant operational challenge.

Initially, the prevailing notion centered around the alternating nature of Bhuban’s strata, oscillating between layers of sandstone and shale. The sand beds, on average, maintain a mere one-meter thickness. However, the sand strata exhibit varying thicknesses, ranging from 10 to 50 cm in locations, due to the lack of vertical connectivity among shale layers within the core of these sand deposits. Identifying exceptional reservoir-grade sandstones within the Bhuban formation is of great importance, especially given the presence of conventional thin beds. This study endeavors to shed light on why the Bhuban Formation offers limited reservoir potential. It seeks to pinpoint distinct facies within the Bhuban formation and characterize them petrographically while assessing the reservoir capabilities of these identified facies types. Thus, three reservoir facies were meticulously examined: Sand Channel, Incised Valley Sand, and Alternation of Shale and Sand. The Sitakunda structure is a box-shaped double-plunging asymmetric anticlinal fold. A reverse fault breaks the western end of the anticline. The Tripura Hills border the structure to the north, the Battali and Patiya Structures to the south, the Halda Syncline and the Semutang Anticline to the east, and the Sandwip Channel to the west (Abdullah et al., 2015). According to a geometrical study projection of 300 readings of

planar structures in the lower hemisphere equal area net, the anticline axis plunges 4° in the $S26^{\circ}E$ direction. The Sitakunda Hill Range, along with other elevated formations in the exposed folded zones of the Bengal Basin, originates from the Upper Bhuban Member from the Miocene period. These formations become visible mainly in road excavations, pedestrian paths, and less accessible tributary areas. The geological arrangement of the area encompasses siltstone and varying shades of sandstone showing light grey, light yellow, and greenish grey, as well as finely laminated to thinly bedded shale and sandy shale in dark grey, bluish-grey, bluish-black, and black hues.

The surveyed sections are the Baridhala road cut segment ($22^{\circ}40'19''$ N, $91^{\circ}38'54''$ E), Chandranath section ($22^{\circ}41'23.7''$ N, $91^{\circ}39'06''$ E), Barabakund section ($22^{\circ}37'52.1''$ N, $91^{\circ}41'06''$ E), and Shastradhara section ($22^{\circ}40'23.6''$ N, $91^{\circ}40'34''$ E). Samples were collected from all four surveyed sections and brought back for laboratory testing and analysis (Fig. 1)

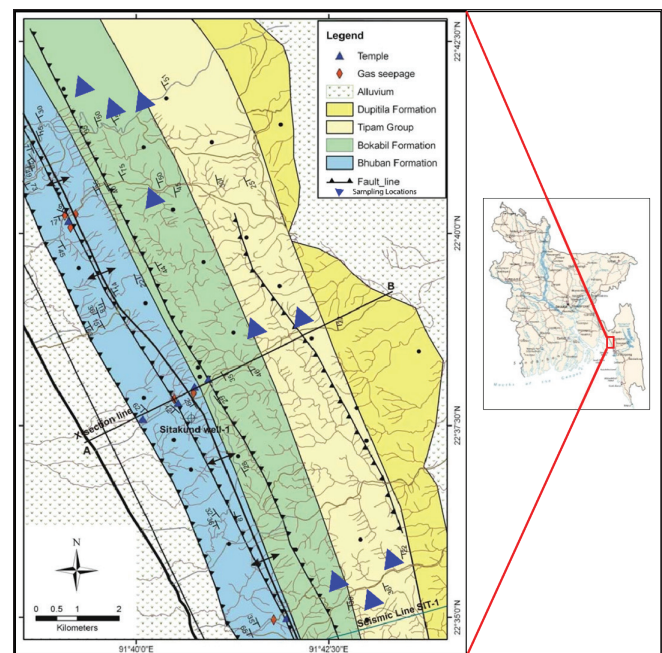


Figure 1: Geological Map of the Sitakunda Area (Modified after Abdullah et al., 2015)

REGIONAL GEOLOGY

The Bengal Basin, an expansive and intricate foreland basin located in the south of the eastern Himalayan Mountains, is a result of the Indian Plate undergoing oblique subduction beneath the Burmese Plate. The east boundary presents additional complexity due to the

right-lateral strike-slip motion occurring along major transform faults such as the Kaladan Fault. Positioned at the northern perimeter of the Surma Basin, there exists a significantly elevated landform referred to as the Shillong Plateau, with an elevation reaching 1750 meters (Curiale et al., 2002). Bangladesh encompasses most of this basin, extending into parts of West Bengal, Assam, Tripura, and Mizoram. Four primary

geotectonic units define the basin's configuration: The Indian Shield to the west, the Shillong Plateau to the north, the Indo-Burman Ranges to the east, and the Bay of Bengal to the south (Hossain et al., 2020) (Fig. 2). Distinct surface anticlines are notably evident within the western segment of the Tripura fold belt. Among the westernmost geological structures within the Bengal Basin fold belt is the Sitakunda anticline.

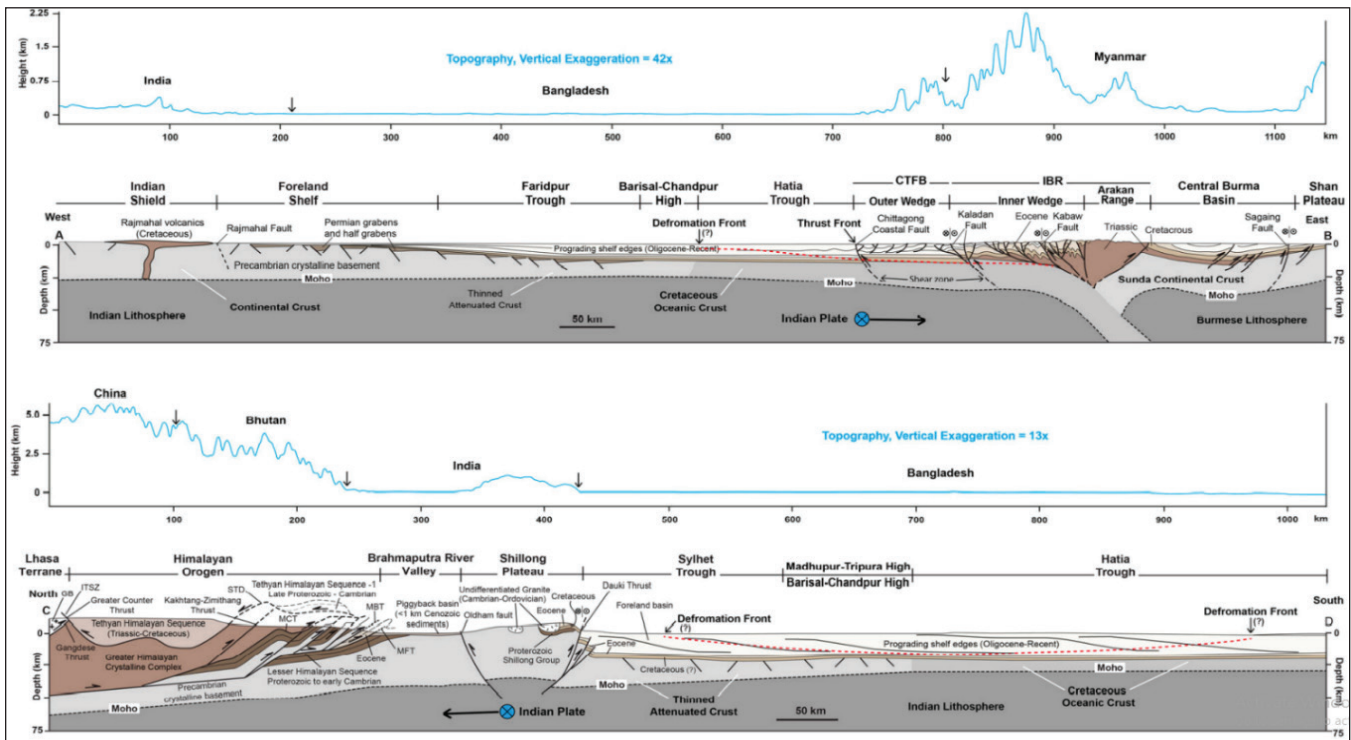


Figure 2: Topographic Profiles and Geological Cross-sections Across the Bengal Basin and Its Surroundings (after Betka et al., 2018; Hossain et al., 2019; Maurin and Rangin, 2009)

A series of anticlines and synclines oriented in the NNW-SSE direction can be observed within the structural zone encompassing Chittagong, the Chittagong Hill Tracts, and the neighboring vicinity. These formations constitute the continuation of the Arakan Yoma Geanticlinal Structure towards the west. The general orientation of the formations in this region aligns closely with that of the Indo-Burman Hill Ranges. Notably, as one moves in a westerly direction, the magnitude of folding and faulting, among other factors, diminishes. This phenomenon suggests that the processes driving the orogenic development of these structures originated on the eastern side.

Much of the extensive geological sequence of Bangladesh comprises Tertiary deposits (Uddin and Lundberg, 2004). The thickness of most units increases as one moves towards the south, and formations that

exhibit deltaic or shallow marine characteristics in the northern regions transition to more marine features in the southern areas (Alam, 1989). In the Bengal Basin, sedimentary layers span from the Paleocene epoch to the Recent period (Najman and Garzanti, 2000). Except for the Sylhet limestone, all other formations consist of clastic deposits. The shale units within the Bokabil and Bhuban formations of the Surma group act as the source of rock for Bangladesh's hydrocarbons (Farhaduzzaman, 2013). The upper Bhuban and Bokabil Formation are home to over 80% of the country's gas reserves (Rahman and McCann, 2012). Interestingly, while the upper sections have garnered less attention, the middle and lower segments of the Bokabil formation have been subjected to comprehensive research endeavors.

Prominent outcrops of the Bhuban and Bokabil formations were evident along the banks of the

Bariyadhala, Sashasradhara, Chandranath temple, and Barabkunda sections, as well as in locations like footpaths, hill cuts, and tributary segments. Exploiting color, overall lithological characteristics, geomorphology, and inferred origin, the Bhuban formation can be categorized into three distinct members: lower, middle, and upper. Shale with modest quantities of sandstone and siltstone prevails in the middle member. The upper member shows sandstone-siltstone formations with a notable presence of shale, while the bottom portion predominantly comprises sandstone-siltstone with substantial shale content. Notably, the lowest member of this anticline remains concealed from view. The middle and upper members measure around 90 to 130 mm and 200 to 260 mm in thickness, respectively.

METHODOLOGY

The study necessitated a series of steps to gather accurate data for interpretation. These steps included an outcrop study, collecting samples, preparing the samples, performing microscopic analysis, scanning electron microscope (SEM) analysis, and conducting X-ray diffraction (XRD).

Outcrop Study

Comprehensive elucidation of the sedimentary structures was utilized to define the features of the outcrops, and the information was documented through basic diagrams and written explanations. In addition to detailing the sediment properties, images of the textures, trends in grain size, coloration, sorting, sphericity, internal arrangements, types of bed connections, and bioturbation were also included.

Sampling and Sample Separation

Sampling was confined to the eastern side of the Sitakund anticline due to its accessibility to most of the Neogene rock formations. At the same time, the western flank is obstructed by faults and concealed by alluvial deposits. Numerous sandstone samples from the designated area were brought to our workshop for further processing, which involved thin section preparation for examination under a microscope, shaping slabs into square forms for scanning electron microscopy (SEM) and isolating shale powder for X-ray Diffraction (XRD) analysis.

Microscopic Analysis

The Research Petrographic Microscope (LEICA) model DM750P enables the observation of various mineral attributes, including color diversity, extinction, twinning, and crystal structure, facilitating the differentiation of distinct mineral varieties. This microscope offers the capability for both optical assessments and capturing sample images. It is equipped with an integrated camera positioned at the top, allowing for video recording and image capture, with the option to save these images directly to a connected computer.

Scanning Electron Microscope (SEM) Analysis

In this examination, the Energy Dispersive Spectrometer (EDS) is employed to produce X-rays from the sample, enabling the assessment of elemental proportions and the identification of minerals. This technique quantifies elements with an accuracy ranging from 0.2 to 1.0 weight percent. This process proved valuable in discerning the morphology of clay and the obstructive influence of clay minerals on pore spaces.

X-ray Diffraction (XRD) Analysis

X-ray Diffraction (XRD) can detect fine-grained minerals, intricate mineral combinations, and interlocking structures that may pose challenges for conventional analytical methods. Beyond fundamental identification, XRD can yield supplementary information. The XRD data can be utilized to ascertain the proportion of each constituent mineral within a composite sample.

RESULTS AND DISCUSSIONS

Outcrop Facies Analysis

This study delineates the depositional systems linked to the Late Miocene Bhuban Formation, drawing insights from outcrop observations. The Shahasradhara-Balukhali, Barabkunda, Chandranath-Microwave, and Bariyadhala sections, collectively serving as representatives, display visible segments of the Bhuban formation. Through thorough field investigations, the recognized facies were systematically grouped into the following classifications: a) Alternating sandstone and shale layers, b) Channel sand, and c) Incised valley sand.

Alternating Sandstone and Shale Layers

The primary facies is characterized by alternating layers of sand and shale. The prevalent sand particles exhibit a light grey hue, range from fine to medium in size, and display a rounded to sub-rounded shape. The thickness of these beds varies between 5 and 50 cm. Initially, in the lower strata, shale thickness surpasses that of sand, but as the succession progresses, the sand-to-shale ratio increases. Within the shale strata, the sands exhibit well-to-moderately sorted characteristics. These sands display a transition from lenticular to wavy configurations as they grade into the adjacent shale layers.

Silt deposits contribute to the formation of a flaser structure, primarily found in the upper portions of ripple troughs and occasionally at the lower part of wave foreset laminae. Sand lenses and laminations are not continuous at the base of the bed; however, they appear flat and parallel towards the upper section. Most of these beds showcase a substantial base, transitioning upwards into parallel laminations, eventually evolving into planar cross-lamination as the configuration changes (Fig. 3).

Channel Sand

The exposed geological formation encompasses channel sands encased within alternating mud-dominant sandstone and shale. These channel sands contribute to a sizeable trough-bedded structure. This structure emerges through clusters of curved or lens-shaped sand deposits within sandstone layers measuring around 0.8 to 2 meters in thickness. Each bed within this configuration ranges from one to two meters in thickness. The sand constituting these trough beds exhibits a medium grain size, a moderately sorted composition, and a yellowish-brown tint. Grains within this sand vary from sub-round to fully round, with grain size generally decreasing in thicker beds. The presence of laminar mud deposits interspersed with lenticular structures featuring mud drapes adds to the complexity of the sand deposit. Notably, the compaction of this sand deposit remains minimal. Moreover, there are no indications of bioturbation impressions on this bed. The exposed unit seems to display a Plano-convex structure (Fig. 4).



Figure 3: Alternating Sand and Shale Layers (facies unit a) Shahasradhara-Balukhali Section

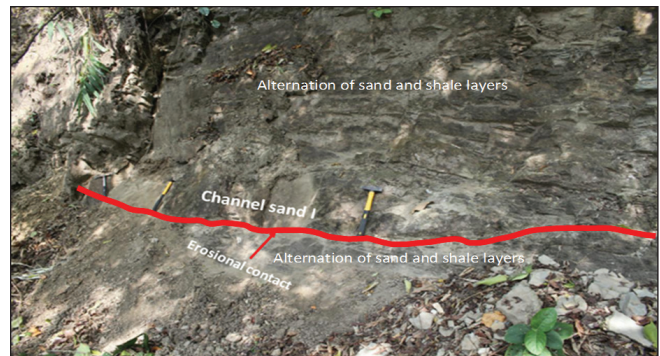


Figure 4: Channel Sand (facies unit b) in Bariyadhala Section (oblique view)

Incised Valley Sand

This particular facies is the most commonly encountered in the field and is present across all sections under study. An erosional boundary distinctly demarcates this facies from facies type “a.” It predominantly comprises large, transparent, and effectively sorted sand particles. The extensive sandstone bed and facies type “a” are closely juxtaposed. The incised valley sand displays a marked association with this scenario. The entirety of the deposit takes on a triangular configuration, with the width and thickness of the incised valley sand varying between 50 and 100 meters and 20 to 50 meters, respectively (Fig. 5).



Figure 5: Incised Valley Sand (facies unit c) in Bariadala Section

Petrographic Study

The research required a thorough petrographic analysis of the collected samples from each distinct facies type. This examination delved into the textural and chemical attributes of the detrital and authigenic components, as unveiled through microscopic sections of the deposits.

Alternating Sandstone and Shale Layers

The Tidal Flat Deposits primarily dictate the grain size, predominantly within the fine-grained category with a minor presence of coarser particles. A majority of the grains display weak to moderate sorting, and they range from sub-angular to sub-rounded, with some appearing sub-prismoidal. An average matrix content of 3 to 4% was observed across most samples. Nevertheless, when considering the grain size, sorting, and matrix content within the sandstone samples, it becomes evident that they predominantly exhibit textural immaturity (Fig. 6).

As indicated by point count data (Fig. 6), quartz constitutes approximately 45% of the entire grain composition, followed by feldspars at 10%, monocrystalline phyllosilicates including mica and chlorite at 25%, and lithic grains contributing to about 10% of the overall grain composition.

The porosity observed in the segment suggests an average porosity of 15%. The predominant grains within the facies are of medium to coarse texture. The presence of concavo-convex, suture, and elongated grain contacts suggests significant compaction has diminished the original porosity of the rock sample. Additionally, the dissolution of cement and quartz has given rise to secondary porosity through chemical processes (Rahman and Worden, 2016) (Fig. 7).

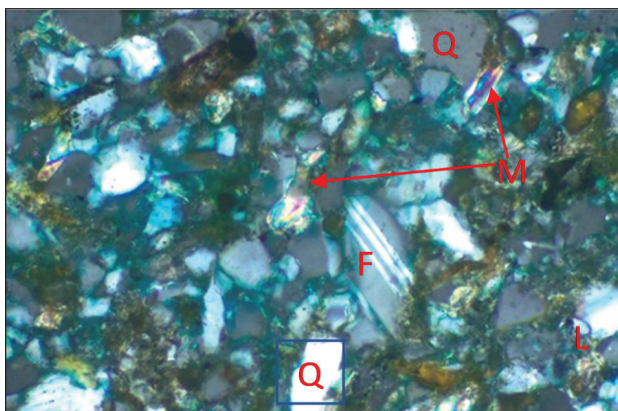


Figure 6: Alteration of Sand and Shale Under Crossed Polarized Light (40X). The Image is Showing Identified Minerals- Quartz (Q), Lithic Grain (L), Mica (M), Feldspar (F) and Matrix

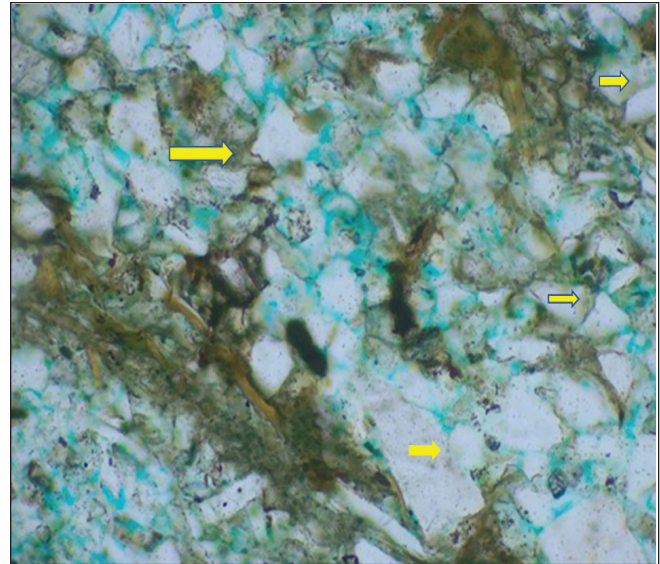


Figure 7: Alteration of Sand and Shale Under Plane Polarized Light (40X). The Image is Showing Porosity in Blue Colours and Grain to Grain Long Contact, Concave-Convex Contact, Point Contact, Suture Contact, Grain Corrosion (Yellow Arrow)

Channel Sand

The grain size observed in channel fill deposits is predominantly medium-grained, with a minor presence of both coarse and fine-grained particles. The majority of the grains display weak to moderate sorting, and they range from subrounded to subprismoidal in shape. An average matrix content of 3% was found in most samples. Nevertheless, when considering the grain size, sorting, and matrix content within the sandstone samples, it becomes evident that they exhibit characteristics of textural immaturity (Fig. 8).

According to point count data (Fig. 8), quartz constitutes approximately 55% of the total grain composition, followed by feldspars at 10%, monocrystalline phyllosilicates such as mica and chlorite at 20%, lithic grains contributing to about 10% of the overall grain composition, and opaque minerals making up roughly 5% of the grains.

The porosity evident in the segment indicates an average porosity level of 20%. The predominant grains within the channel sand facies are fine to medium size, exhibit a moderately sorted arrangement, and contain minimal matrix content. Concavo-convex, suture, lengthy contacts (Fig. 9), and mica bending (Fig. 10) indicate substantial compaction, reducing porosity. However, corroded grains (Fig. 9) suggest that both the cement

and grains have undergone chemical dissolution, thereby fostering the development of secondary porosity (Rahman and Worden, 2016).

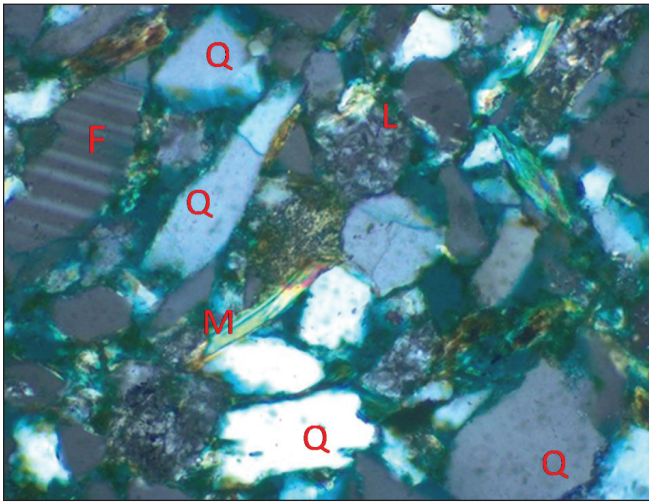


Figure 8: Channel Sand Under Crossed Polarized Light (40X). The Image is Showing Identified Minerals-Quartz (Q), Lithic Grain (L), Mica (M), Feldspar (F) and Matrix

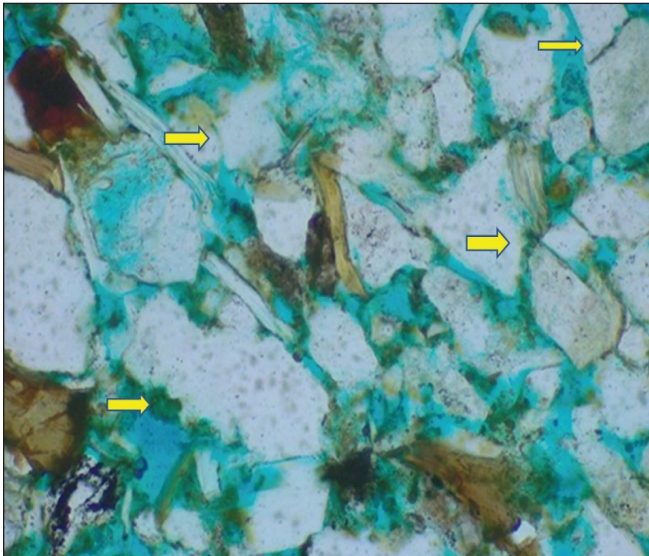


Figure 9: Channel Sand Under Plane Polarized Light (40X). The Image is Showing Porosity in Blue Colour and Grain to Grain Long Contact, Concavo-Convex Contact, Point Contact, Grain Corrosion (Yellow Arrow)

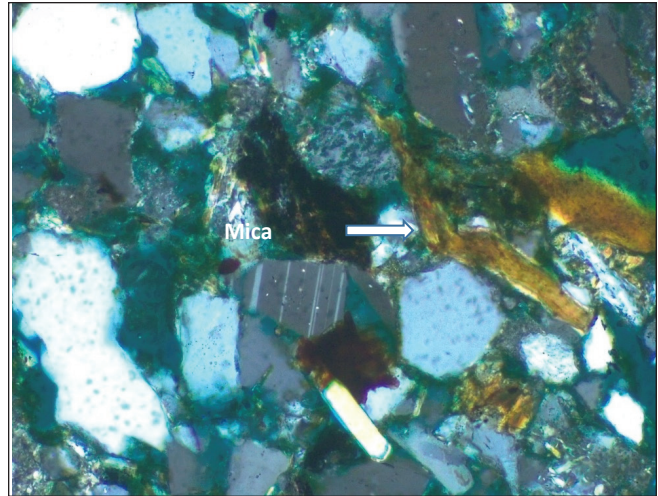


Figure 10: Channel Sand Under Crossed Polarized Light (40X). The Image is Showing Mica Bending

Incised Valley Sand

The prevailing grain size is predominantly in the medium to coarse range. Most grains exhibit moderate to well-organized sorting, appearing sub-rounded and sub-prismoidal in shape, consistent with the characteristics of Tidal flat deposits. Most samples show a matrix content of 2 to 4%. However, the grain size, sorting, and matrix content within the sandstone samples collectively suggest their predominantly texturally immature nature (Figs. 11 and 12).

According to point count data (Fig. 11), quartz constitutes approximately 65% of the total grain composition, followed by feldspars at 10%, monocrystalline phyllosilicates like mica and chlorite at 10%, lithic grains contributing to about 10% of the overall grain composition, and opaque minerals accounting for roughly 5% of the grains.

The porosity observed within the segment indicates an average porosity of 25%. The detrital and authigenic elements comprising the Incised Valley sand are predominantly coarse-grained and well-sorted and feature limited matrix content. The interlocking nature of the grains within the rock sample is not particularly distinct. The rock has undergone substantial compaction, evidenced by a few extended and concavo-convex contacts. However, notable chemical dissolution of the cement and grains has resulted in the development of considerable secondary porosity (Fig. 13).

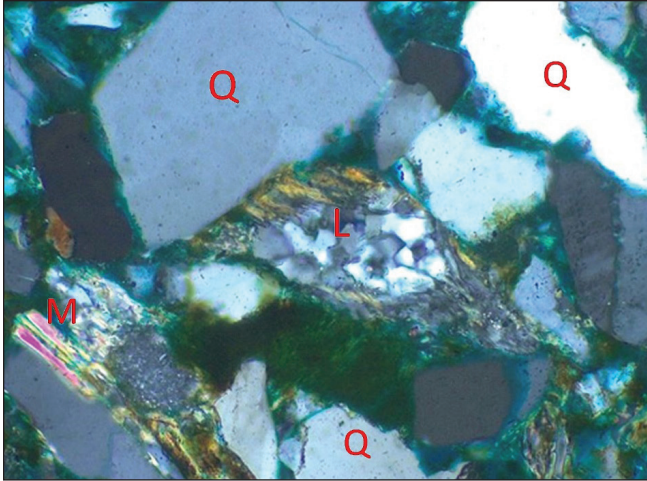


Figure 11: Incised Valley Sand Under Crossed Polarized Light (40X). The Image is Showing Identified Minerals- Quartz (Q), Lithic Grain (L), Mica (M)

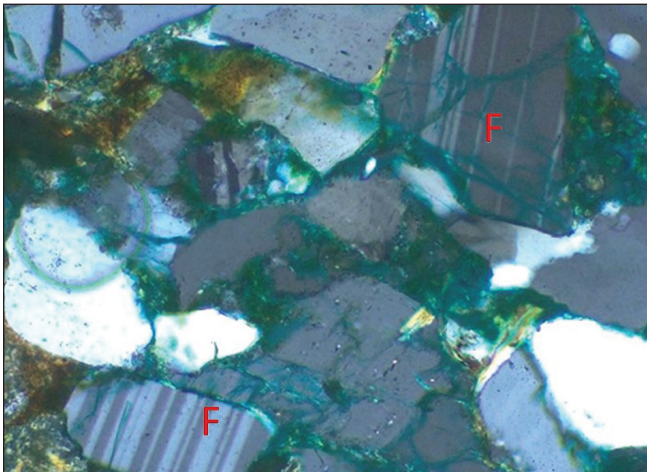


Figure 12: Incised Valley Sand Under Crossed Polarized Light (40X). The Image is Showing Identified Feldspar (F)

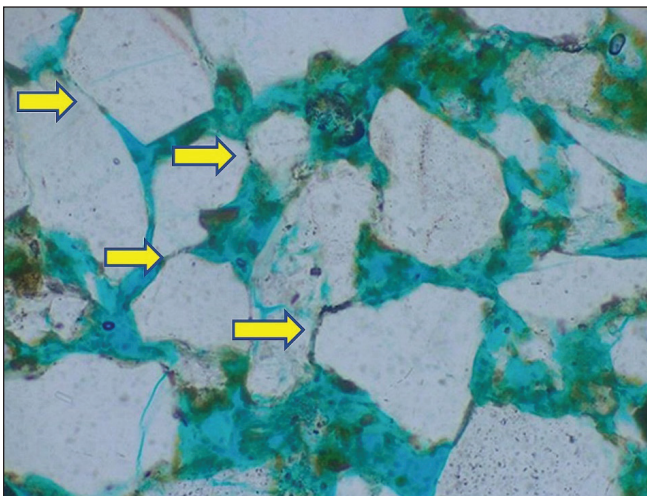


Figure 13: Incised Valley Sand Under Plane Polarized Light (40X). The Image is Showing Porosity in Blue

Colour and Grain to Grain Long Contact, Concavo-Convex Contact, Point Contact by Yellow Arrow Sign

X-ray Diffraction (XRD) Analysis

Alternating Sandstone and Shale Layers

The XRD analysis reveals both bulk and oriented clay samples and demonstrates that the clay lenses predominantly consist of kaolinite, with minor illite, smectite, and biotite. In XRD analysis, the presence of illite is identified by its dispersed reflection pattern.

Specifically, illite is recognized by its peaks at 2-theta (deg) values of 8.924 and 17.827, with corresponding intensities of 98 and 42 counts. Kaolinite is identified by its peak at a 2-theta (deg) value of 12.552, exhibiting an intensity of 92 counts. Smectite is determined by its peak at a basal spacing of 6.304 2-theta (deg), with an intensity of 48 counts. Quartz is detected at two distinct basal spacing values: 20.9 and 26.671 2-theta (deg), with intensities of 87.2 and 503 counts, respectively. Notably, the intensity of quartz at 26.671 is higher than that at 20.9. Finally, feldspar is identified by its peak at a basal spacing of 27.963 2-theta (deg), with an intensity of 51 counts (Fig. 14).

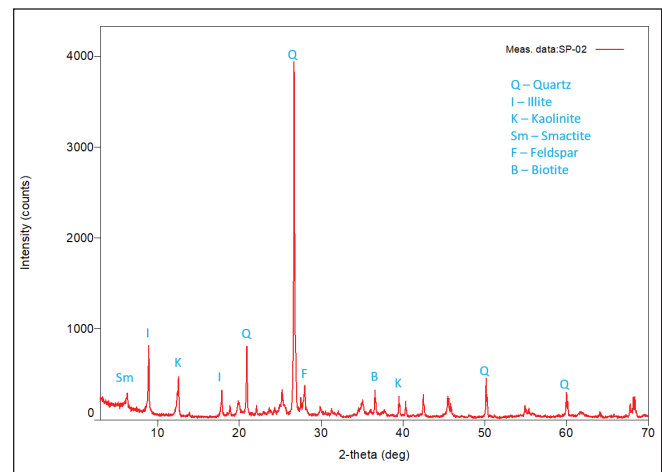


Figure 14: X-Ray Diffraction (XRD) Curve (2-theta (deg) vs Intensity (counts)) of Alternation of Sand Shale Layer Sample Showing Different Minerals-Mectite, Illite, Kaolinite, Quartz, Biotite, Feldspar

Channel Sand

Illite presence is confirmed by its characteristic peaks

at basal spacings of 8.853 and 17.755, corresponding to 2-theta (deg) values, with intensities of 58.8 and 24.2 counts, respectively. The identification of kaolinite is marked by a peak at a 2-theta (deg) value of 12.497, exhibiting an intensity of 63.6 counts. Smectite's recognition is indicated by its peak at a basal spacing of 6.19, corresponding to 2-theta (deg), with an intensity of 28.4 counts. Quartz is detected at two basal spacings: 20.831 and 26.608, with intensities of 104 and 511 counts, respectively. Notably, the intensity of quartz at 26.608 surpasses that of the previous one. Finally, feldspar is confirmed by its peak at a basal spacing of 27.930, corresponding to 2-theta (deg), with an intensity of 115 counts (Fig. 15).

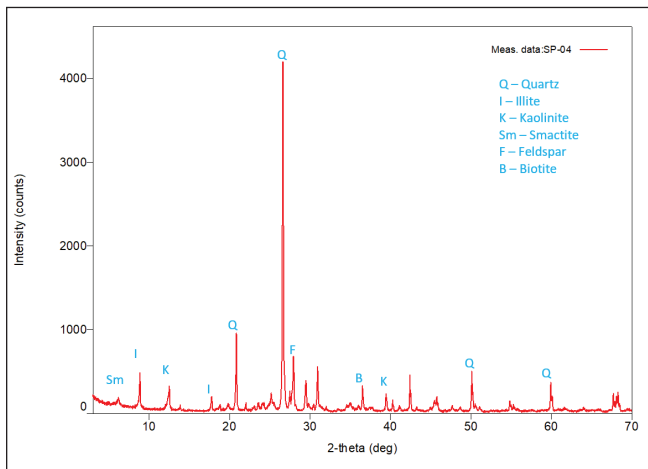


Figure 15: X-Ray Diffraction (XRD) Curve (2-theta (deg) vs Intensity (counts)) of Channel Sand Sample Showing Different Minerals – Smectite, Illite, Kaolinite, Quartz, Biotite, Feldspar

Incised Valley Sand

Illite is distinguished by its recognizable peaks at basal spacings of 8.850 and 17.775, corresponding to 2-theta (deg) values and exhibiting intensities of 53.5 and 20.5 counts, respectively. Kaolinite is detected through its distinctive peak at a 2-theta (deg) value of 12.474, displaying an intensity of 84.9 counts. The presence of smectite is indicated by its peak at a basal spacing of 6.23, corresponding to 2-theta (deg), and an intensity of 22.1 counts. Quartz is identified at two basal spacings: 20.837 and 26.605, with intensities of 110 and 526 counts, respectively. Notably, the intensity of quartz at 26.605 surpasses that of the previous one. Lastly, the presence of feldspar is confirmed by its peak at a basal spacing of 27.884, corresponding to 2-theta (deg), with an intensity of 93 counts (Fig. 16).

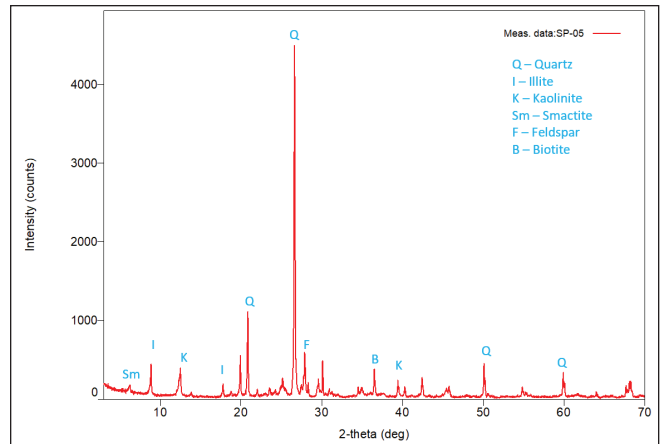


Figure 16: X-Ray Diffraction (XRD) Curve (2-theta (deg) vs Intensity (counts)) of Incised Valley Sand Sample Showing Different Minerals-Smectite, Illite, Kaolinite, Quartz, Biotite, Feldspar

Scanning Electron Microscope (SEM) Analysis

Alternating Sandstone and Shale Layers

Due to the inclusion of clay minerals within the pore spaces, the porosity is not continuous but is significant. The abundance of kaolinite is evident, characterized by its plate-like grain structure. The gaps between quartz grains have been occupied, and a coating is observed on the grains. The porosity demonstrates a maximum radius of 2 to 2.5 micrometers (Fig. 17).

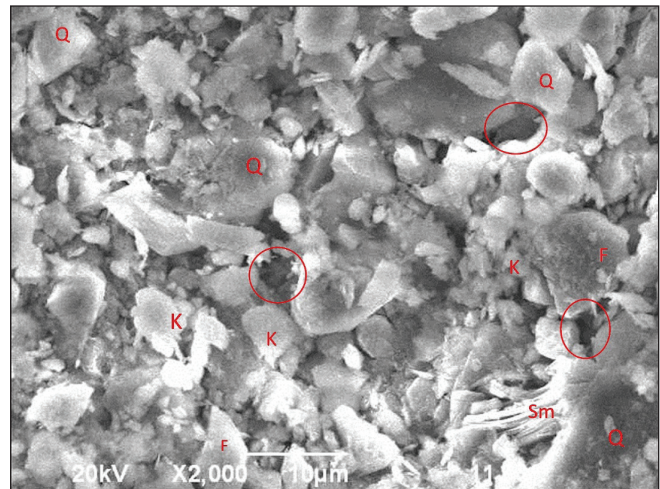


Figure 17: Scanning Electron Microscope (SEM) Image of Alternation Sand Shale Layers Showing Quartz (Q), Kaolinite (K), Feldspar (F), Smectite (Sm) and Porosity with Red Circle

Channel Sand

Additionally, there is considerable interconnected porosity. The grains vary in size, spanning from medium to coarse. There are a limited number of clay minerals, predominantly plate-shaped kaolinite. The continuity of pore space has been disrupted, possibly due to the movement of kaolinite particles. The porosity exhibits a maximum radius of 4 to 5 micrometers (Fig. 18)

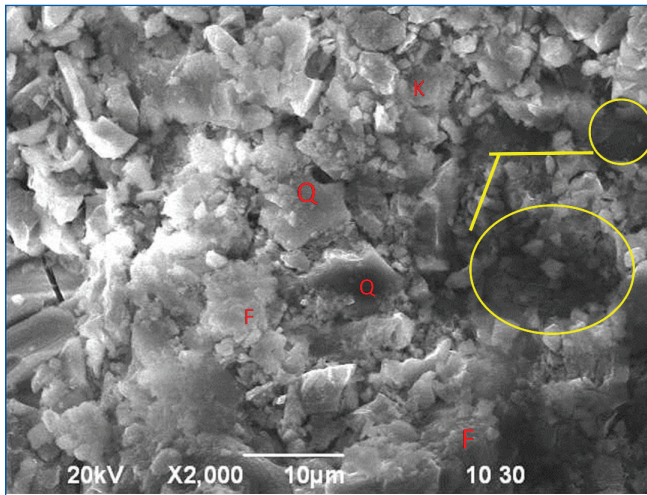


Figure 18: Scanning Electron Microscope (SEM) Image of Channel Sand Showing Quartz (Q), Kaolinite (K), Feldspar (F) and Porosity with Yellow Circle

Incised Valley Sand

Predominantly, coarse-grained sands are observed, and they exhibit significant porosity. Minor quantities of clay material have facilitated the enlargement and effective interconnection of the porosities. The porosity demonstrates a maximum radius of 10 to 12 micrometers (Fig. 19).

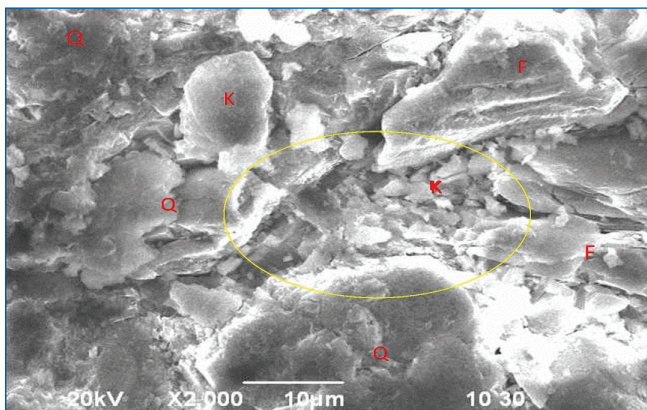


Figure 19: Scanning Electron Microscope (SEM) Image

of Incised Valley Sand Showing Quartz (Q), Kaolinite (K), Feldspar (F) and Porosity with Yellow Circle

CONCLUSIONS

Within the Bhuban formation, three distinct facies types are predominant: alteration of sand and shale, channel sand, and incised valley sand. Among these, the alteration of the sand-shale layer is the most widespread facies identified during the field investigations. In contrast, the other two facies, incised valley sand and channel sand, were encountered less frequently and in isolated sections. The sand-shale layer alteration demonstrates poor sorting characteristics, primarily fine-grained composition, and notable porosity. Channel sand exhibits medium to coarse particle size, moderate sorting, and good porosity. Sand originating from an incised valley displays well-organized sorting, a predominantly coarse-grained texture, and a notable porosity level. These facies distinctions have been established through meticulous petrographic analyses and comprehensive outcrop assessments.

The XRD analysis revealed the presence of diverse clay minerals within the samples. As the sand shale layers transitioned into channel sand and incised valley sand, the intensity of different clay minerals declined. Conversely, the intensities of quartz and feldspar showed a consistent increase. SEM analysis disclosed the presence of clay minerals in the first sample, predominantly kaolinite, which impeded pore space and disrupted porosity connectivity. In contrast, channel sand and incised valley sand showcased fewer clay constituents. Within the channel sand sample, we identified moderate-sized porosity with satisfactory interconnectivity, while in the incised valley sand sample, we encountered larger-sized porosity with exceptional connectivity.

In summary, the findings lead to the conclusion that the alteration of the sand shale layer does not represent a favorable reservoir. In contrast, channel sand can be considered a reasonably suitable reservoir, and incised valley sand emerges as the most promising reservoir. Given the substantial transformation of sand and shale strata, the overall assessment suggests that the Bhuban Formation has a limited reservoir potential.

REFERENCES

- Abdullah, R., Yeasmin, R., Mahbulul Ameen, S.M., Khanam, F. and Bari, Z., 2015. 2D structural modelling and hydrocarbon potentiality of the Sitakund structure, Chittagong Tripura Fold Belt, Bengal Basin, Bangladesh. *Journal of the Geological Society of India*, 85, pp.697-705.
- Alam, M., 1989. Geology and depositional history of Cenozoic sediments of the Bengal Basin of Bangladesh. *Palaeogeography, Palaeoclimatology, Palaeoecology*, 69, pp.125-139.
- Alam, M., Alam, M.M., Curray, J.R., Chowdhury, M.L.R. and Gani, M.R., 2003. An overview of the sedimentary geology of the Bengal Basin in relation to the regional tectonic framework and basin-fill history. *Sedimentary geology*, 155(3-4), pp.179-208.
- Alam, M.M., Curray, J.R., 2003. The curtain goes up on a sedimentary basin in south-central Asia: unveiling the sedimentary geology of the Bengal Basin of Bangladesh. *Sedimentary Geology*, 3(155), pp.175-178.
- Basri, R., Woobaidullah, A.S.M., Hossain, D., Bhuiyan, M.A.H., 2023. Outcrop analogy with the subsurface geology and hydrocarbon prospectivity of Jaintiapur and adjacent areas in North-East Bangladesh. *Journal of Natural Gas Geoscience*, 8(1), pp.63-93.
- Betka, P.M., Seeber, L., Thomson, S.N., Steckler, M.S., Sincavage, R., Zoramthara, C., 2018. Slip-partitioning above a shallow, weak décollement beneath the Indo-Burman accretionary prism. *Earth and Planetary Science Letters*, 503, pp.17-28.
- Bhuiyan, M. A. H., 1995. Petrographic characterization and interpretation of Neogene Surma Group sandstone of Sitakund structure, Chittagong, Bangladesh. Unpubl. M. Sc. thesis, Geology Dept., Dhaka University, Bangladesh, 152pp
- Brindley, G.W., 1952. Identification of clay minerals by X-ray diffraction analysis. *Clays and Clay Minerals*, 1, pp.119-129.
- Curiale, J.A., Covington, G.H., Shamsuddin, A.H.M., Morelos, J.A., Shamsuddin, A.K.M., 2002. Origin of petroleum in Bangladesh. *AAPG bulletin*, 86(4), pp.625-652.
- Evans, P., 1932. Tertiary succession in Assam. *Trans. Min. Geol. Inst. India*, 27(3), pp.155-260.
- Farhaduzzaman, M., 2013. Characterization of selected petroleum source rocks and reservoir rocks of Bengal Basin (Bangladesh) based on geochemical, petrographical and petrophysical methods. University of Malaya (Malaysia).
- Farhaduzzaman, M., Islam, M.A., Abdullah, W.H., Islam, M.S., 2015. Petrography and diagenesis of the Tertiary Surma Group reservoir sandstones, Bengal Basin, Bangladesh. *Universal Journal of Geoscience*, 3(3), pp.103-117.
- Gani, M.R., Alam, M.M., 2003. Sedimentation and basin-fill history of the Neogene clastic succession exposed in the southeastern fold belt of the Bengal Basin, Bangladesh: a high-resolution sequence stratigraphic approach. *Sedimentary Geology*, 155(3-4), pp.227-270.
- Hossain, M.S., Xiao, W., Khan, M.S.H., Chowdhury, K.R., Ao, S., 2020. Geodynamic model and tectono-structural framework of the Bengal Basin and its surroundings. *Journal of Maps*, 16(2), pp.445-458.
- Hossain, M.S., Khan, M.S.H., Chowdhury, K.R., Abdullah, R., 2019. Synthesis of the tectonic and structural elements of the Bengal Basin and its surroundings. *Tectonics and structural geology: Indian context*, pp.135-218.
- Imam, B., 2013. Energy resources of Bangladesh: natural gas. Oil, Coal, University Grants Commission of Bangladesh, Dhaka, Bangladesh.
- Islam, M.R., Lupin, J.H., 2020. A review on hydrocarbon prospectivity in Chittagong Hill tracts and adjacent area. *Open Journal of Geology*, 10(2), pp.187-212.
- Maurin, T., Rangin, C., 2009. Structure and kinematics of the Indo-Burmese Wedge: Recent and fast growth of the outer wedge. *Tectonics*, 28(2).
- Najman, Y., Garzanti, E., 2000. Reconstructing early Himalayan tectonic evolution and paleogeography from Tertiary foreland basin sedimentary rocks, northern India. *Geological Society of America Bulletin*, 112(3), pp.435-449.
- Noh, J.H., Lee, I., 1999. Diagenetic pore fluid evolution in the Pohang Miocene sediments: oxygen isotopic evidence of septarian carbonate concretions and

- authigenic mineral phases. *Geosciences Journal*, 3, pp.141-149.
- Rahman, M.J.J., McCann, T., 2012. Diagenetic history of the Surma group sandstones (Miocene) in the Surma Basin, Bangladesh. *Journal of Asian Earth Sciences*, 45, pp.65-78.
- Rahman, M.J.J., Worden, R.H., 2016. Diagenesis and its impact on the reservoir quality of Miocene sandstones (Surma Group) from the Bengal Basin, Bangladesh. *Marine and Petroleum Geology*, 77, pp.898-915.
- Reimann, K.U., Hiller, K., 1993. *Geology of Bangladesh*.
- Tucker, M. E., 2009. *Sedimentary petrology: an introduction to the origin of sedimentary rocks*. John Wiley & Sons, 272pp
- Uddin, A., Lundberg, N., 2004. Miocene sedimentation and subsidence during continent–continent collision, Bengal basin, Bangladesh. *Sedimentary Geology*, 164(1-2), pp.131-146.
- Zou, C., Zhu, R., Liu, K., Su, L., Bai, B., Zhang, X., Yuan, X., Wang, J., 2012. Tight gas sandstone reservoirs in China: characteristics and recognition criteria. *Journal of Petroleum Science and Engineering*, 88, pp.82-91.